

Progress Report eRD19 - Detailed Simulations of Machine Background Sources and the Impact to Detector Operations (January 2017)

January 6, 2017

Project ID: eRD19

Project Name: Detailed Simulations of Machine Background Sources and the Impact to Detector Operations

Period Reported: from October 2016 to January 2017

Project Leader: Elke Aschenauer

Contact Person: Elke Aschenauer, Richard Petti

Project members: BNL physics: Elke-Caroline Aschenauer, Alexander Kiselev, Richard Petti; BNL-CAD: Christoph Montag, Robert Palmer, Vadim Ptitsyn, Dejan Trbojevic; BNL-Magnet Division: Brett Parker

Abstract

This document describes the progress made since the original proposal on the R&D efforts on simulating machine generated backgrounds and the impact on the environment in which the detectors must operate and analyses must be done. The focus of this period is simulating background generated from beam-gas interactions, taking into account realistic machine configurations and parameters for the case of eRHIC. Expected rates of backgrounds, along with maps of where the detectors are hit by background particles are reported. A calculation estimating the probability of having physics events overlap with background events in the detector is also shown.

1 Past

The goal of this period of review (beginning October 2016) is to begin investigations and simulations of machine generated backgrounds and to continue the valuable collaboration and communication with the accelerator department at Brookhaven. The focus in this period of review is on beam-gas interactions and estimation and characterization of this background in multiple design scenarios for eRHIC. Although the specifics of the study are tailored to eRHIC, the developed tools can be used for any experimental setup or facility.

1.1 Beam-gas simulations

Beam-gas interactions can be a significant source of background in the detectors and need to be mitigated when doing an analysis at an EIC. Beam-gas interactions occur when the beam particles collide with residual gas particles inside the beam pipe vacuum. The focus here is on the dominant contribution from the proton beam interacting with gas in the beam pipe. A simulation and assessment has been done, assuming various scenarios for the machine design parameters. This is compared to rates expected from physics from e+p collisions.

The base of the simulation is dpmjet3 [1]. Dpmjet3 is a Monte Carlo package that can simulate e+A and p+A collisions. After conversing with the vacuum group at RHIC, it was determined that the dominate gas present in the beam pipe at RHIC is H² to the 90% level. Thus this study begins with simulating p+H² collisions. Simulations with p+Ar to simulate the remaining contributions from heavier gas molecules have also been performed, but are not yet incorporated into the current calculation.

The p+H² simulations are generated with a 250 GeV proton beam with a fixed target H² nuclei ($\sqrt{s_{NN}} = 21.7$ GeV). The particle species produced in the collisions, along with their frequency of production in terms of per event yield, is shown in Fig. 1. As may be expected, most of the particles produced are pions, followed by protons and neutrons.

All events produced in Dpmjet3 are produced at the origin at the IP. To get a realistic sense of the configuration and geometry of the collisions and associated background particles, the vertex of each collision is displaced. This is accomplished with an after-burner code that transforms the original output of Dpmjet3 to an event record with a displaced vertex. The event vertex points are distributed along the beam orbit path, determined from a standalone beam particle sent through the GEANT implementation of the experiment (EicRoot). At the moment, the gas density along the beam path is assumed to be uniform, thus the generated vertex distribution is uniform along the beam pipe. The orientation of the proton in the orbit (i.e. the angle with respect to the z-axis) is also taken into account and is reflected in the modified event record.

After the events are given displaced vertices, the events are then fed into the detector and IR simulation package EicRoot [2], which has been used to great success in eRD12. Any IR setup can easily be imported into the simulation with a simple ASCII file description

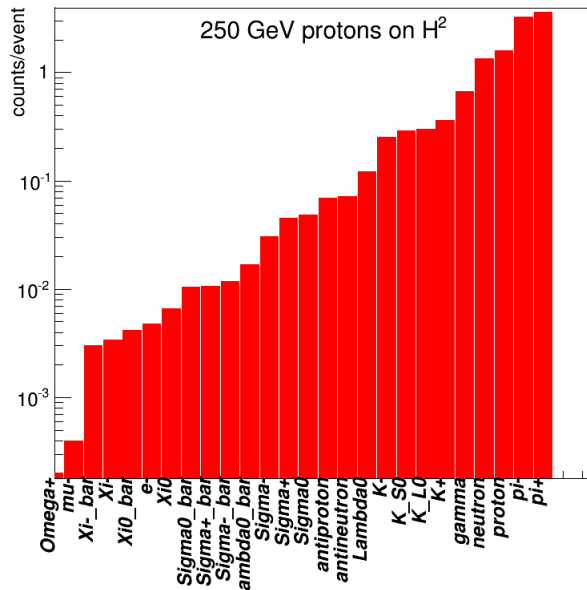


Figure 1: The per event rate of various particle species produced in 250 GeV proton collisions with fixed target H^2 simulated with Dpmj3.

of the magnet locations, apertures, and field/gradients in the magnets. The current study focuses on using two different IR lattice setups obtained by C-AD at BNL, the linac-ring based setup (currently on version 3) and the recirculating ring-ring based setup (currently on version 2). For reference, the magnet layout for the designs under consideration are shown in Fig. 2. The magnet layout has only been designed for the forward region after the detector (pushed by the Roman Pot acceptance studies from eRD12). Given the lack of a detailed design in the backward region (in front of the detector from the incoming proton beam perspective) needed for this study, the magnet layouts shown in Fig. 2 have been reflected about the interaction point. This is a reasonable approximation to what will be designed in the future.

The generated particles are tracked through the corresponding magnet lattice. Particles that enter into the main detector volume are identified as any particle that has a space point simultaneously within $|z| < 4.5$ m and outside the beampipe radius of 2 cm.

Figures 3 and 4 (left) show a hit map of the particles that enter into the main detector region as a function of the particle (or event) vertex in x and z (z is along the proton beam at the IP) for the linac-ring and ring-ring setups respectively. The boxes in the figure represent the magnet apertures for reference. The right side of the figures show a hit map as a function of the event vertex in z and the individual particle energy. Note that these simulations currently ignore secondary particles generated by interaction with the magnet structures present in the IR (though interaction with air in the detector cave is allowed).

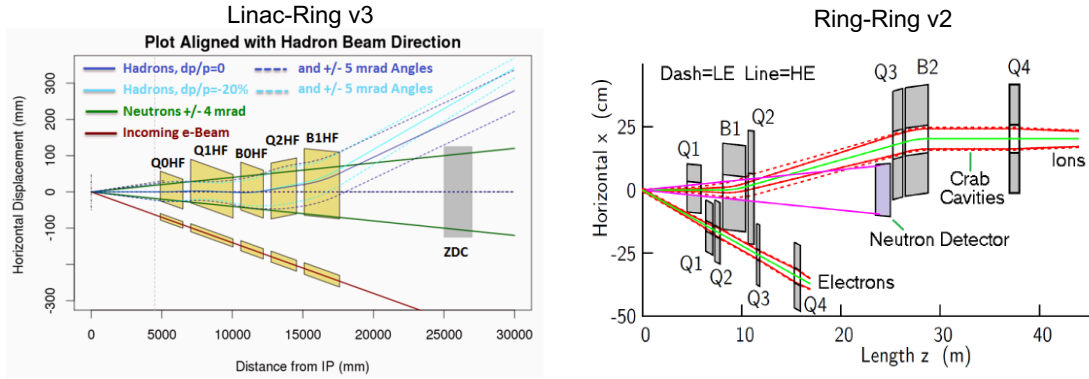


Figure 2: Schematics of the interaction region designs used for the study obtained by BNL C-AD for the Linac-Ring (left) and Ring-Ring (right) concepts.

The next iteration of the study will take these effects into account. The figures show that most of the background events that produce particles that make it into the detector originate after the magnets and within the detector beampipe (though this statement is not as strong for the Ring-ring design).

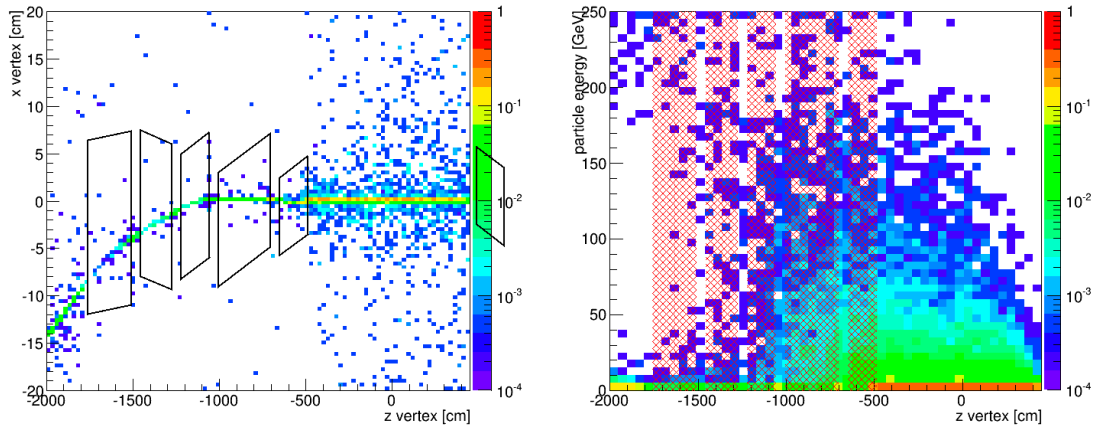


Figure 3: A hitmap of particles from background $p+H^2$ events entering the detector area as (left) a function of the particle vertex in x and z ; (right) a function of the particle vertex in z and the particle energy for the linac-ring v3 IR setup.

Figures 5 and 6 show where the particles from the background events will enter the detector, broken into bins of the background particle vertex position in z . This is important, since it needs to be understood what specific detectors systems will have the most burden from these background events.

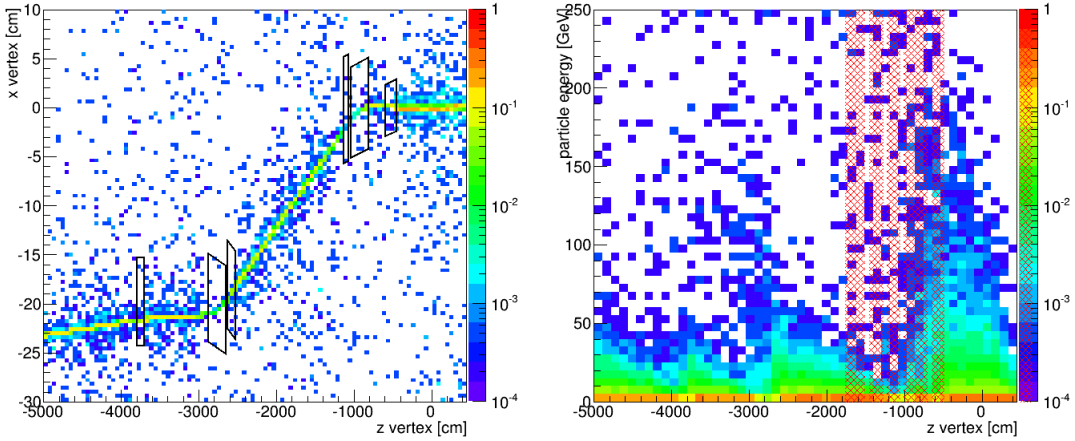


Figure 4: A hitmap of particles from background $p+H^2$ events entering the detector area as (left) a function of the particle vertex in x and z ; (right) a function of the particle vertex in z and the particle energy for the ring-ring v2 IR setup.

Please note that in Figs. 3 - 6, that the simulated range along the beam line is different for the Linac-ring and Ring-ring designs. Since the Ring-ring design features magnets that are further from the detector compared to the Linac-ring plan, the generated vertex range has been extended from -20 m to -50 m to get the best possible view of the entire designed IR region. One feature apparent in the hit distributions is the square shaped hole (most notably viewed in Fig. 6). This is due to the magnet bulk implemented in the simulation. Particles can hit the detector by either going around the magnet or going through the aperture in the magnet, resulting in the shape observed.

It is essential to properly normalize the particle rates coming from the simulation to model reality in terms of the beam parameters for the machine design options. This normalization is achieved by estimating the expected luminosity of the background collisions combined with the expected production cross section of the interaction. For a fixed target experiment, the luminosity can be determined from Eqn. 1.

$$L = \Phi \cdot \rho \cdot l \quad (1)$$

In Eqn. 1, L is the luminosity, Φ is the particle flux ($\Phi = N_p/s$), ρ is the target density, and l is the length of gas assumed in the simulation. The particle flux can be estimated from the proton beam current under the operation of that specific design. Table 1 summarizes the relevant quantities for the different accelerator designs and proton beam parameters. For these calculations, the assumed gas density is 10^{-9} mbar (or 2.65×10^7 molecules/cm³). This is the vacuum that has been achieved at HERA and is a reasonable benchmark for these studies. Discussions are underway with the vacuum group at RHIC

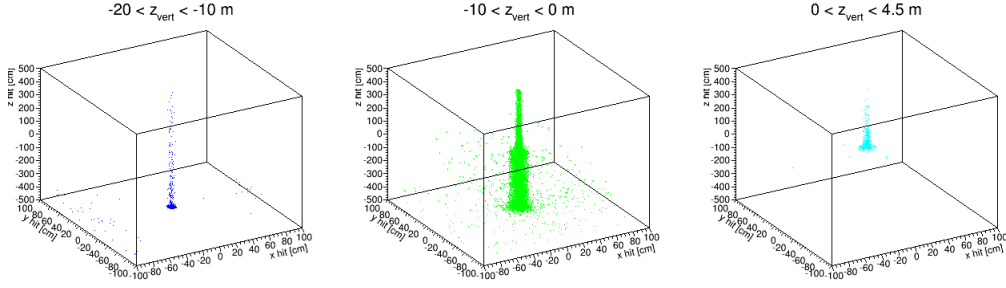


Figure 5: A hitmap of particles from background $p+H^2$ events entering the detector area at the first point of entry into the detector for the Linac-ring design. The separate panels show the hit distribution for particles originating in collisions in particular z vertex bins as labeled.

Machine Design	Rep. Rate [MHz]	Beam energy (e+p) [GeV]	Proton current [mA]	Background Lumi [$\times 10^{25} \text{ cm}^{-2} \text{ s}^{-1}$]
Linac-ring (low risk)	9.4	13 x 275	415	7.5
Linac-ring (ultimate)	9.4	8.3 x 250	415	7.5
Ring-ring (baseline)	28.2	10 x 250	460	8.3
Ring-ring (ultimate)	114	10 x 250	937	16.9

Table 1: A table summarizing the relevant machine quantities and the associated luminosity of background events. The gas density is assumed to be the same as at HERA, roughly 10^{-9} mbar or 2.65×10^7 molecules/cm³.

to determine the vacuum in the IR at RHIC, along with looking into the time dependence of the vacuum.

Table 2 shows the comparison of the interaction cross-section for the background $p+H^2$ (250 GeV proton on fixed target H^2) collisions and the $e+p$ collisions (10 x 250 GeV), along with the associated luminosity for the interactions. It is observed that the cross-section for $p+H^2$ collisions is roughly two orders of magnitude greater than that for the $e+p$ collisions. This is cause for concern. Because of this it is critical to have an excellent vacuum (to reduce the luminosity of the background interactions) combined with the methods to increase the machine luminosity without significantly increasing the beam current (i.e. cooling methods to shrink the beam).

The particle distributions obtained from the aforementioned Dpmjet3 simulations are then scaled by the expected rates (calculated by multiplying the luminosity by the cross section) summarized in Table 3 for each of the machine design options. A comparison to the rates expected from DIS simulated with Pythia [3], is also shown and summarized in

Machine Design	p+H ² cross section [mb]	Background Lumi [x 10 ²⁵ cm ⁻² s ⁻¹]	e+p cross section [mb]	Machine Lumi [x 10 ³³ cm ⁻² s ⁻¹]
Linac-ring (low risk)	60	7.5	0.05	1.2
Linac-ring (ultimate)	60	7.5	0.05	14.4
Ring-ring (baseline)	60	8.3	0.05	1.1
Ring-ring (ultimate)	60	16.9	0.05	12.4

Table 2: A table summarizing the cross sections for the background physics, DIS physics, and the associated luminosities for the process.

Machine Design	Background rate [kHz]	DIS rate [kHz]	Physics/BG ratio
Linac-ring (low risk)	11	58	5.3
Linac-ring (ultimate)	11	700	64
Ring-ring (baseline)	24.5	53	2.2
Ring-ring (ultimate)	55.6	603	11

Table 3: A table summarizing the expected rates for background and DIS events for the different machine options.

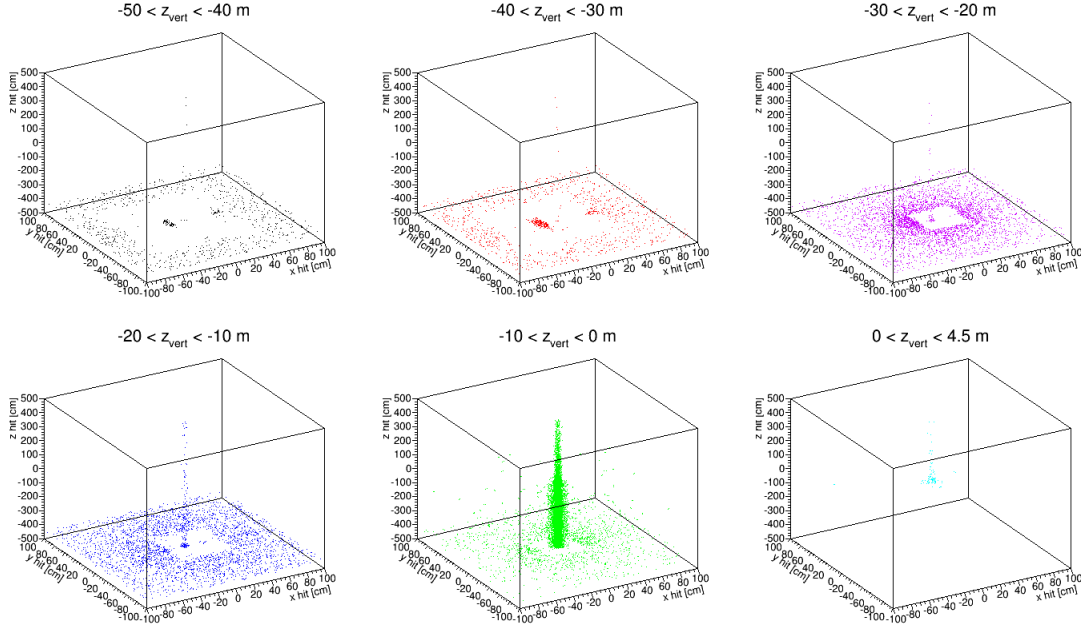


Figure 6: A hitmap of particles from background $p+H^2$ events entering the detector area at the first point of entry into the detector for the Ring-ring design. The separate panels show the hit distribution for particles originating in collisions in particular z vertex bins as labeled.

the table, along with the ratio of the rates. The normalized particle spectra as a function of energy is shown in Figs. 7 and 8.

Of interest to this study is the probability that a DIS event will be spoiled by the presence of background particles polluting the event. This is estimated and described below.

To estimate the probability of event overlap, the proportion of generated background events that have particles that enter the detector area within an event gate timing window (currently estimated as 10 ns) is calculated. Thus in this approach, it is assumed that a DIS event occurred within this event gate. The time it takes the particles from a background event to enter the detector area is estimated by assuming every particle travels at the speed of light and the distance is estimated as a straight line path to the point of detector entry. The calculation needs to be further adjusted for the relative rate of DIS to background events to model the actual probability of collision in a bunch in each case. The results for each machine design is summarized in Table 4.

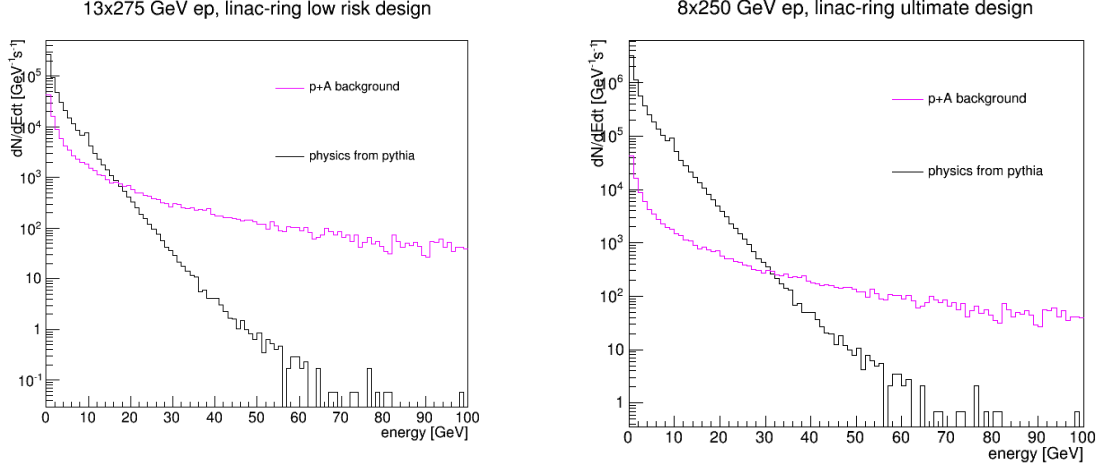


Figure 7: A comparison of the particle distributions normalized for realistic event rates from background beam-gas events (magenta) to DIS events (black) for the Linac-ring design (left: baseline, right: ultimate).

2 Future

The next period of review will refine some of the details in the beam-gas studies presented here. Namely, the contribution from secondary particles produced from interaction with structures in the IR will be evaluated, including backscatter from magnet elements on the forward side of the detector. The same diagnostics are also expected to be performed for lower beam energies. Additional contributions from heavier gas molecules will also be studied. A more differential look into the composition of particle species hitting different areas of the detector will also be studied.

Secondly, studies related to synchrotron radiation background in the detector will also

Machine Design	Event overlap probability (>1 particle)	Event overlap probability (>5 particles)
Linac-ring (low risk)	0.10	0.08
Linac-ring (ultimate)	0.008	0.006
Ring-ring (baseline)	0.2	0.09
Ring-ring (ultimate)	0.04	0.02

Table 4: A table summarizing the expected rates for background and DIS events for the different machine options.

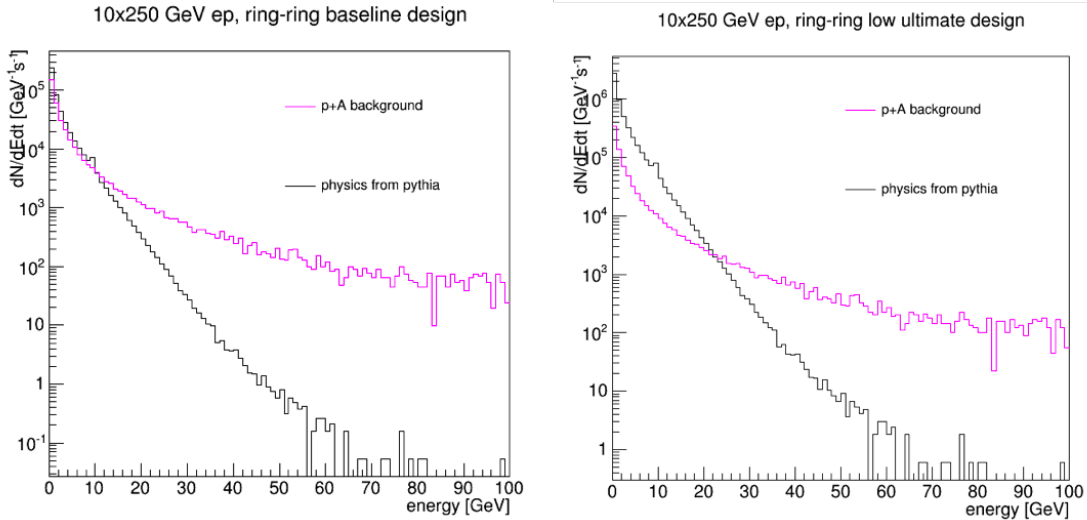


Figure 8: A comparison of the particle distributions normalized for realistic event rates from background beam-gas events (magenta) to DIS events (black) for the Ring-ring design (left: baseline, right: ultimate).

be performed. Discussions have already begun with the members of C-AD.

3 Manpower

Manpower working on the project is summarized below, listed in alphabetical order, but separated by department.

- Elke Aschenauer - BNL physics. Provides project guidance and is the supervisor of the project.
- Alexander Kiselev - BNL physics. Provides software support.
- Richard Petti - post-doc at BNL working under the supervision of Elke Aschenauer. Performed the bulk of the work and works on the project full time.
- Christoph Montag - BNL-CAD. Provides the magnet design for the interaction region for the ring-ring machine design.
- Robert Palmer - BNL-CAD. Provides the magnet design for the interaction region for the ring-ring machine design.
- Brett Parker - BNL-CAD/Magnet division. Provides the magnet design of the interaction region for the linac-ring machine design.

- Vadim Ptitsyn - BNL-CAD. Provides project guidance.
- Dejan Trbojevic - BNL-CAD. Provides project guidance through expertise in the machine lattice design.

References

[1] <https://wiki.bnl.gov/eic/index.php/DPMJet>.

[2] <https://wiki.bnl.gov/eic/index.php/Eicroot>.

[3] <https://wiki.bnl.gov/eic/index.php/PYTHIA>.